

# ON THE POSSIBLE ASSOCIATION OF ULTRA HIGH ENERGY COSMIC RAYS WITH NEARBY ACTIVE GALAXIES

IGOR V. MOSKALENKO<sup>1</sup> AND ŁUKASZ STAWARZ<sup>2</sup>

Kavli Institute for Particle Astrophysics and Cosmology, Stanford University, Stanford, CA 94309

TROY A. PORTER

Santa Cruz Institute for Particle Physics, University of California, Santa Cruz, CA 95064

AND

CHI C. CHEUNG

NASA Goddard Space Flight Center, Astrophysics Science Division, Code 661, Greenbelt, MD 20771

*Draft version November 11, 2018*

## ABSTRACT

Data collected by the Pierre Auger Observatory (Auger) provide evidence for anisotropy in the arrival directions of cosmic rays (CRs) with energies  $>57$  EeV that suggests a correlation with the positions of active galactic nuclei (AGN) located within  $\sim 75$  Mpc and  $3.2^\circ$  of the arrival directions. This analysis, however, does not take into account AGN morphology. A detailed study of the sample of AGN whose positions are located within  $3.2^\circ$  of the CR events (and extending our analysis out to  $\sim 150$  Mpc) shows that most of them are classified as Seyfert 2 and low-ionization nuclear emission-line region (LINER) galaxies whose properties do not differ substantially from other local AGN of the same types. Therefore, if the production of the highest energy CRs is persistent in nature, i.e., operates in a single object on long ( $\gtrsim$  Myr) timescales, the claimed correlation between the CR events observed by Auger and local active galaxies should be considered as resulting from a chance coincidence. Additionally, most of the selected sources do not show significant jet activity, and hence, in most conservative scenarios, there are no reasons for expecting them to accelerate CRs up to the highest energies,  $\sim 10^{20}$  eV. If the extragalactic magnetic fields and the sources of these CRs are coupled with matter, it is possible that the deflection angle is larger than expected in the case of a uniform source distribution due to effectively larger fields. A future analysis has to take into account AGN morphology and may yield a correlation with a larger deflection angle and/or more distant sources. We further argue that the nearby radio galaxy NGC 5128 (Cen A) alone could be associated with at least 4 events due to its large radio extent, and PKS 1343–60 (Cen B), another nearby radio galaxy, can be associated with more than 1 event due to its proximity to the Galactic plane and, correspondingly, the stronger Galactic magnetic field the ultra high energy CRs (UHECRs) encounter during propagation to the Earth. If the UHECRs associated with these events are indeed accelerated by Cen A and Cen B, their deflection angles may provide information on the structure of the magnetic field in the direction of these putative sources. Future  $\gamma$ -ray observations (by, e.g., *Fermi Gamma-ray Space Telescope* [Fermi] formerly *Gamma-Ray Large Area Space Telescope* [GLAST], and *High Energy Stereoscopic System* [HESS] in the Southern hemisphere) may provide additional clues to the nature of the accelerators of the UHECRs in the local Universe.

*Subject headings:* cosmic rays — galaxies: active — galaxies: individual (Cen A, Cen B, PKS 2158–380, PKS 2201+044) — intergalactic medium

## 1. INTRODUCTION

The spectrum, origin, and composition of CRs at the highest energies ( $\geq 10^{18}$  eV  $\equiv 1$  EeV; hereafter UHECRs) has been a puzzle since their discovery almost 50 years ago (for a review see Cronin 2005; Nagano & Watson 2000). The isotropy of the arrival directions of UHECRs above  $10^{18}$  eV suggests an extragalactic origin, though Galactic objects such as fast rotating neutron stars with ultrastrong magnetic fields (“magnetars”) are capable of accelerating particles up to  $\sim 10^{20}$  eV (Hillas 1984). The UHECR energy losses due to photopion production on the cosmic microwave background (CMB) – the so-called GZK effect (Greisen 1966; Zatsepin & Kuz’mين 1966) – mean that the sources of the highest energy particles should be cosmologically close, within  $\sim 100$  Mpc. However, observations of the spectrum at these high energies are ex-

tremely challenging due to the low overall event rate ( $\sim 1$  per  $\text{km}^2$  per century at  $\sim 10^{20}$  eV). Fine structure in the CR spectrum above  $10^{18}$  eV has been predicted (e.g., Berezhinsky et al. 2006) – the GZK cutoff, a pile-up bump, and a dip due to photoproduction of pairs – and indeed found in experiments, but the interpretation is not straightforward due to the large uncertainty in the source distribution, their injection spectrum, and CR chemical composition.

Quite a few extragalactic objects discussed in the literature are potentially capable of accelerating UHECRs. Among those are shocks from the epoch of the large scale structure formation,  $\gamma$ -ray bursts, galaxy clusters, AGN (in particular, those AGN with powerful jets) and powerful AGN flares (Farrar & Gruzinov 2008), the lobes of giant radio galaxies (Stanev 2007a), and newly born magnetars in other galaxies (Ghisellini et al. 2008); various exotic top-down scenarios have also been discussed but seem unlikely (e.g., Abraham et al. 2007a, 2008b). Extragalactic jets and their extended radio lobes have been proposed

<sup>1</sup> Also Hansen Experimental Physics Laboratory, Stanford University, Stanford, CA 94305

<sup>2</sup> Also Astronomical Observatory, Jagiellonian University, ul. Orla 171, 30-244 Kraków, Poland

as one of the most likely acceleration sites of UHECRs (e.g., Biermann & Strittmatter 1987; Dermer 2007; Ostrowski 2002, and references therein). In this paper we, therefore, will follow the “jet paradigm”, i.e. assume that UHECR particle acceleration takes place in jets or is associated with them. However, not all AGN have jets, and for those that do the jet properties may differ substantially between different classes/types (see a discussion in §2).

There are also quite a few “known unknowns” which affect the distribution of the arrival directions of UHECRs and make the association with particular classes of objects a non-trivial task. Among these are the source distribution, the structure of extragalactic and Galactic magnetic fields, the nature of sources (transient vs. steady), and the energy spectrum and chemical composition at injection (we discuss these topics in §4).

The Auger Collaboration has reported significant evidence for anisotropy in the arrival directions of UHECRs (Abraham et al. 2007b, 2008a). The anisotropy signal suggests a correlation of the events with AGN listed in the Véron-Cetty & Véron (2006) catalog with distances less than  $\sim 100$  Mpc, though other sources with a similar distribution are not ruled out<sup>3</sup>. The maximum correlation has been found for AGN with redshift  $z \leq 0.017$  (corresponding distance  $D \leq 71$  Mpc), angular separation  $\theta \leq 3.2^\circ$ , and events with energy above  $\sim 57$  EeV. The list of events with energy in excess of 57 EeV consists of 27 events, and 20 of these correlate with the AGN from the Véron-Cetty & Véron (2006) catalog.

In this paper we discuss the possible association between UHECRs and AGN based on a detailed analysis of a selected sample of nearby active galaxies contained within the  $\theta \leq 3.2^\circ$  search radius of the UHECR events detected by Auger, drawn from the Véron-Cetty & Véron (2006) catalog, with additional AGN taken from the NASA/IPAC Extragalactic Database (NED). Our study of the properties of the selected sample of AGN, described here in detail, shows that it consists predominantly of low-luminosity sources such as Seyfert galaxies and LINERs, and a handful of radio galaxies.

In §2 we give a brief introduction (not intended as a comprehensive review) into the AGN phenomenology targeting non-expert readers; those familiar with the AGN background material could safely skip it. In §3 we discuss a sample of local AGN selected using exactly the same criteria ( $\theta \leq 3.2^\circ$  and  $z \leq 0.018$ ) for each UHECR event that correspond to the maximum significance of the correlation reported by the Auger Collaboration. We extend the search out to redshifts  $z \leq 0.037$  which doubles the distance to 150 Mpc, and effectively covers the range of horizons for super-GZK particles (Abraham et al. 2008a; Harari et al. 2006). With such a sample, we investigate the properties of the listed 54 active galaxies. In particular, we address the two following issues: (i) Are the selected objects different in any respect from the other numerous local AGNs? (ii) Are they in general able to accelerate cosmic rays to ultra high energies? Based on the selection criteria, we identify four powerful radio galaxies which could be potential sources of, at least, 7 out of 27 reported UHECR events. We complete with the discussion of the propagation of UHECRs from the sources to the observer (§4), and argue that the correlation radius between the arrival direction of UHECRs and the sources could be significantly larger than  $\theta \leq 3.2^\circ$  found by the Auger Collaboration

and depends on the UHECR source distribution and the assumed model of intergalactic and Galactic magnetic fields. In §5 we summarize our reasoning that the observed correlation is most probably chance coincidence given the high density of low power AGN in the local universe.

## 2. PHENOMENOLOGY OF LOCAL AGN

A number of weak AGN in the local Universe can be observed and even resolved due to their proximity which allows a broad range of AGN activity to be studied, while only bright ones can be seen at large distances. At the current state of our knowledge, however, not all AGN types could be recognized as potential sources of UHECR. A brief introduction into the types of AGN activity is, therefore, warranted as a basis for further discussion.

### 2.1. Nuclei

Supermassive black holes ( $M_{\text{BH}} \sim 10^6 M_\odot - 10^9 M_\odot$ ) are found in a number of galaxies, and there is growing consensus that all galaxies contain accreting black holes at their centers. If the emission of the accreting/circumnuclear matter is pronounced, the galaxy is classified as active. Such emission includes a non-stellar blue continuum due to the accretion disk and strong, but narrow, forbidden emission lines resulting from photoionization of the surrounding gas by the disk radiation. It has been shown that about 85% of all galaxies (and, in particular, almost all nearby late-type galaxies) possess detectable emission-line nuclei, which therefore could be classified as AGN (Ho 2008). In most cases, however, the nuclear luminosity is very weak relative to the stellar radiative output of the host galaxy<sup>4</sup>. These nearby low-luminosity AGN can be divided into Seyfert galaxies ( $\gtrsim 10\%$  of local AGN) and LINERs ( $\sim 60\%$ ), depending on the ionization level and intensity of the emission lines<sup>5</sup>. For more details we refer the reader to the recent review by Ho (2008).

The rest of the local AGN assemblage is populated by radio galaxies (mostly low-power ones of the FR I type; Fanaroff & Riley 1974) and BL Lacertae objects (BL Lacs). In these sources, the radiative output of the accreting/circumnuclear gas (which may, spectroscopically, resemble closely the Seyfert or LINER types) is dominated, or at least substantially modified, by a broad-band non-thermal emission produced by relativistic jets emanating from the active centers. Also, radio galaxies and BL Lacs are hosted almost exclusively by giant elliptical and S0 galaxies, while the majority of Seyferts and LINERs ( $\gtrsim 90\%$ ) are associated with spiral galaxies (e.g., Bahcall et al. 1997; Malkan et al. 1998; Martel et al. 1999). Therefore, Seyferts/LINERs and FR Is/BL Lacs are *morphologically different* and this may have important consequences/implications for their capability of accelerating particles to the highest observed energies, as discussed in the next section.

Some fraction of AGN exhibit in addition broad permitted emission lines ( $\text{FWHM} \sim 10^3 - 10^4 \text{ km s}^{-1}$ ) in their spectra; the presence/absence of such lines divides further the AGN population into type 1/type 2 classes. In the framework of the “AGN unification scheme”, these two classes are intrinsically identical, and differ only in the orientation of the

<sup>4</sup> If the nuclear emission outshines the starlight of the host galaxy, the source is classified as a quasar.

<sup>5</sup> We note that the starburst nuclei of many galaxies, as well as their H II regions, also possess ionization lines, which are, however, weaker than the ones observed in Seyferts or LINERs, and are photoionized exclusively by the starburst activity.

<sup>3</sup> Note that the Auger Collaboration acknowledges the incompleteness of the catalog and does not make any serious claims concerning source classes.

accretion disk symmetry axis to the line of sight (Antonucci 1993). Namely, type 1 AGN are thought to be predominantly observed at small inclination angles (roughly  $<40^\circ$ ), while type 2 AGN are viewed at larger angles through a high-column-density gas and dust concentrated at pc-scale distances from the active center in a torus-like structure (coplanar with the inner accretion disks). As a result, the disk continuum and broad emission lines produced very close to supermassive black holes are heavily obscured in type 2 AGN, but not in type 1 sources. The narrow line emission, originating at larger distances ( $> \text{pc}$ ) from the active center, is not subjected to strong obscuration.

Such a unifying picture is supported by several observational findings, including detections of strong mid-infrared (MIR) emission due to the dusty obscuring tori in basically all different classes and types of AGN. In addition to the MIR/optical/UV non-stellar nuclear radiation, Seyferts and LINERs show characteristic X-ray emission extending from 0.1 keV up to 100 keV photon energies with photon indices  $\Gamma_X \lesssim 2.0$ , which is probably produced within the hot coronae of the accretion disks (see, e.g., Svensson 1996; Zdziarski 1999). The low-energy ( $< 2 \text{ keV}$ ) segment of this continuum is typically obscured in type 2 sources, which agrees with the unification scheme. We also note that in the framework of the unification paradigm, all BL Lacs are considered to be simply low-luminosity radio galaxies (FR Is) viewed at very small viewing angles ( $\lesssim 10^\circ$ ) to the jet axis.

## 2.2. Jets

Acceleration of particles to ultrarelativistic energies in AGN is observationally confirmed (through detection of the intense non-thermal emission) to be associated with collimated fast jets, which are produced by the active black hole/accretion disk systems<sup>6</sup>, or in shocks created by a propagating jet. The strong magnetization, extremely low density, non-stationary relativistic and supersonic flow pattern, and finally turbulent character of such jets (see, e.g., the review by Begelman et al. 1984), is expected to result in the formation of non-thermal particle energy distributions extending up to the highest accessible energies. Indeed, the very high energy  $\gamma$ -ray emission detected from blazars<sup>7</sup>, demonstrates the ability of the nuclear (sub-pc scale) relativistic AGN outflows to efficiently accelerate electrons up to 1 – 100 TeV energies (e.g., Celotti & Ghisellini 2008). In the case of large (kpc)-scale jets, as observed in powerful radio galaxies and radio-loud quasars, it has been speculated that proton energies in the 10 – 100 EeV range can be reached as well (e.g., Lyutikov & Ouyed 2007; Ostrowski 1998).

Not all AGN are jetted. Also, it seems that only some fraction of nuclear jets can remain relativistic and well-collimated during the propagation through the dense environments of the central parts of host galaxies. These issues are particularly relevant for Seyferts and LINERs, which differ substantially from the bona fide jet sources like radio galaxies and radio-loud quasars, lacking in particular well-defined large-scale jet structures. We also note in this context, that no galaxy classified as Seyfert or LINER has been detected so far at  $\gamma$ -ray

( $> \text{MeV}$ ) energies<sup>8</sup>.

The jet production and acceleration efficiency may depend on the *morphology* of the host galaxy. Sikora et al. (2007) proposed that the difference in the efficiency of the jet production between spiral-hosted AGN (Seyfert galaxies and LINERs) and elliptical-hosted ones (low-power FR I radio galaxies, their more powerful analogs classified as FR II radio sources, BL Lacs, quasars) may be explained if the spin of the central supermassive black holes,  $J$ , in spiral galaxies is on average lower than in elliptical ones. According to the so-called “spin paradigm”, the efficiency for the production of relativistic jets in AGN depends on the spin of the supermassive black hole (Blandford 1990). This has been investigated in detail by Volonteri et al. (2007), who, by means of numerical simulation, confirmed that indeed the cosmological evolution of supermassive black holes is expected to lead to such a host morphology-related spin dichotomy. If true, this may have important consequence for the acceleration of CRs to the highest observed energies. Namely, the electromotive force of the black hole embedded in an external magnetic field  $B$  (supported by the accreting matter) is  $\Delta V \sim B r_g (J/J_{\text{max}})$  (e.g., Phinney 1983), where  $J_{\text{max}} = c r_g \mathcal{M}_{\text{BH}}$  is the maximum value of the black hole spin, and  $r_g$  is the gravitational radius of the black hole. Assuming further that the magnetic energy density close to the black hole event horizon is equal to the energy density of the matter accreting at the Eddington rate, the maximum energy a test particle with an electric charge  $Ze$  can reach in such a potential drop is  $E_{\text{max}} \sim Ze \Delta V \sim 3 \times 10^{20} Z (\mathcal{M}_{\text{BH}}/10^8 \mathcal{M}_\odot)^{1/2} (J/J_{\text{max}}) \text{ eV}$ . If this picture is correct then many (most) of the local low-power AGN with  $\mathcal{M}_{\text{BH}} < 10^8 \mathcal{M}_\odot$  and accreting at sub-Eddington rates, and are additionally characterized by  $J \ll J_{\text{max}}$  as expected in the case of the spiral-hosted Seyferts/LINERs, may not have enough potential to accelerate CRs to ultra high energies (Hopkins & Hernquist 2006; Sikora et al. 2007; Volonteri et al. 2007).

Jet activity always manifests itself as non-thermal synchrotron radio emission produced by ultrarelativistic jet electrons. Hence, investigation of jet properties are usually addressed by detailed radio studies. In the case of local AGN, like Seyferts and LINERs, such studies are hampered due to the low luminosities and small sizes of the radio structures. Additionally, most of these sources, and in principle all local spiral-hosted AGN, show intense star formation activity (especially pronounced in the far-infrared [FIR]), see, e.g., Ho (2008). Such activity is known for producing the radio-emitting outflows due to starburst-driven superwinds which, although completely different in origin, may in some (morphological and spectral) respects closely resemble jet-related activity. Thus, care must be taken when making any statement regarding jet properties in these objects with limited radio data.

The synchrotron/jet origin of the compact cores observed in local low-luminosity AGN is supported by the direct detections of nuclear jets in these systems (Kukula et al. 1999; Middelberg et al. 2004; Ulvestad et al. 1998). Interestingly, observations of the proper motions of such structures indicate sub-relativistic bulk velocities on sub-pc/pc-scales,

<sup>6</sup> Note, that there is no observational evidence for a significant population of non-thermal particles in AGN accretion disks and disk coronae. In fact, hard X-ray/soft  $\gamma$ -ray emission observed from Seyferts is best modeled assuming a thermal population of electrons, albeit characterized by high temperatures of the order of 100 keV.

<sup>7</sup> Blazar class includes BL Lacertae objects and radio loud quasars with flat spectrum radio cores.

<sup>8</sup> This may change with the next generation of  $\gamma$ -ray satellites (*Fermi*/Large Area Telescope [*Fermi*/LAT]) and ground-based Cherenkov Telescopes (such as the next phases of HESS, *Major Atmospheric Gamma-ray Imaging Cherenkov telescope* [MAGIC], or *Very Energetic Radiation Imaging Telescope Array System* [VERITAS]).

$v < 0.25c$  (Middelberg et al. 2004; Ulvestad et al. 1999a,b). Note that the observed brightness temperatures of the radio cores in Seyferts and LINERs, as well as their moderate year-timescale variability, do not require relativistic beaming (Mundell et al. 2000). Also, the observed one-sidedness of nuclear jets in these systems is best explained as resulting from free-free absorption of radio photons on the surrounding gaseous disks, and not due to relativistic (Doppler) effects (Middelberg et al. 2004). This constitutes a clear difference with the established properties of radio galaxies and quasars.

We also emphasize that the distribution of nuclear jets in Seyferts and LINERs is random with respect to the host galaxy stellar disks (Kinney et al. 2000; Nagar & Wilson 1999; Pringle et al. 1999; Schmitt et al. 2001, 2002; Thean et al. 2001). Moreover, misalignments between sub-pc/pc-scale jets and kpc-scale radio structures are common in Seyferts, being much larger than those observed in other radio-loud AGN (Colbert et al. 1996; Gallimore et al. 2006; Kharb et al. 2006; Middelberg et al. 2004). The misalignment angle distribution is flat over the whole range  $0^\circ$  to  $90^\circ$  (Middelberg et al. 2004). This may suggest that kpc-scale radio structures are not powered by the jets, but rather originate in starforming regions. Such an interpretation is sometimes supported by the fact that the extended radio-emitting halos in some Seyferts and LINERs are aligned with the galaxy disks, and that their radio powers correlate with the FIR fluxes as observed in regular spiral and starforming galaxies (Thean et al. 2001).

However, in most of the cases ( $\geq 45\%$ ) the observed kpc-scale radio structures of Seyferts and LINERs do not morphologically match those of galaxy disks or starforming regions, showing also excess radio emission over the radio-FIR correlation (Gallimore et al. 2006; Kharb et al. 2006). Thus, such structures are believed to be powered directly by jets, which are, however, substantially different from the ones observed in other radio-loud AGN. In particular, there is growing consensus that Seyferts and LINERs are characterized by short-lived low-power jet activity epochs, with jet lifetimes  $t_j \lesssim 10^5$  yrs and jet kinetic luminosities  $L_j \sim 10^{41} - 10^{43}$  erg  $s^{-1}$ , possibly triggered by minor accretion episodes, which repeat every  $\sim 10^6$  yrs in different (random) directions over the whole Seyfert-type activity epoch  $\lesssim$  Gyr (Capetti et al. 1999; Gallimore et al. 2006; Kharb et al. 2006; Sanders 1984).

### 2.3. Radio activity

Radio surveys of local Seyferts and LINERs provide further insight into the nature of their activity and reveal typically complex, multi-component radio structures, consisting of compact unresolved or slightly resolved cores (detected at centimeter wavelengths in most of these objects), linear jet-like features (observed in  $\sim 30\%$  of the local low-luminosity AGN), and spherical or elongated diffuse halos/radio bubbles (present in, again,  $\sim 30\% - 50\%$  of the Seyfert and LINER population; e.g., Baum et al. 1993; Colbert et al. 1996; Gallimore et al. 2006; Ho & Ulvestad 2001; Morganti et al. 1999; Rush et al. 1996; Ulvestad & Wilson 1989). The total radio power of these objects at centimeter wavelengths is in the range  $\sim 10^{35} - 10^{42}$  erg  $s^{-1}$  (with median value  $L_{5\text{ GHz}} \sim 2 \times 10^{37}$  erg  $s^{-1}$ ; Ho & Ulvestad 2001), which is typically slightly higher than the total radio luminosities of “regular” spiral galaxies.

For the compact cores of Seyfert and LINERs, previously no dependence in radio power or spectral properties on the AGN type (type 1 vs. type 2) or host galaxy mor-

phology (ellipticals vs. spirals) was found (Morganti et al. 1999; Nagar et al. 1999; Rush et al. 1996; Ulvestad & Wilson 1989). However, more recently it has been suggested that the small fraction of those Seyferts which are elliptical-hosted, and possibly also type 1 Seyferts, are characterized by relatively stronger nuclear radio activity (Nagar et al. 2005; Thean et al. 2001; Ulvestad & Ho 2001). Nevertheless, it is established that flat-spectrum radio cores can be present in all types of local low-luminosity AGN, and therefore (unlike in the case of radio galaxies and quasars) cannot be used as a good proxy for the source inclination.

It has been speculated that the flat-spectrum radio cores of Seyferts may not be due to jet activity, but rather some other processes like a nuclear starburst, or the emission of the accretion disks/obscuring tori themselves (e.g., Gallimore et al. 1997). However, the relatively high brightness temperatures of the Seyfert radio cores,  $10^7 \text{ K} < T_b < 10^9 \text{ K}$ , points to a synchrotron (and therefore jet-related) origin of the radio emission (Middelberg et al. 2004; Mundell et al. 2000; Nagar et al. 2005). This is supported by the excess radio emission of the local low-luminosity AGN with detected radio cores over the radio-FIR correlation established for regular spirals and starforming galaxies (Ho & Ulvestad 2001; Roy et al. 1998) which is expected to hold if the radio emission is exclusively/predominantly due to starforming activity (Condon et al. 2002; Helou et al. 1985). Also, recently found scaling relations between the nuclear radio emission of Seyferts and LINERs and their accretion power (approximated by either the  $2 - 10$  keV luminosity of the disk corone, non-stellar optical magnitudes of the active nuclei, or  $H_\beta$  or O III line luminosities), indicate a strong link between the radio production efficiency and the accretion disk parameters, as expected in the case of a jet origin for the radio emission (Ho 2002; Ho & Peng 2001; Panessa et al. 2006, 2007).

### 3. AGN SAMPLE

We collected AGN which are possibly associated with the UHECR events by searching *both* the NASA Extragalactic Database (NED)<sup>9</sup> and the Véron-Cetty & Véron (2006) catalog. We also extend the search out to redshifts  $z \leq 0.037$  ( $\leq 150$  Mpc) which doubles the distance at which maximum significance was found by the Auger Collaboration ( $z \leq 0.018$ ,  $\leq 75$  Mpc); this effectively covers the range of horizons for super-GZK particles (Abraham et al. 2008a; Harari et al. 2006).

Table 1 lists the AGN found within the  $3.2^\circ$  search radius around each UHECR event reported by Auger (Abraham et al. 2008a), divided into two groups: those within redshift range  $z \leq 0.018$  and  $0.018 < z \leq 0.037$  (corresponding approximately to the luminosity distances  $d_L \leq 75$  Mpc and  $75 \text{ Mpc} \leq d_L \leq 150$  Mpc, respectively, Table 2). In total, we have selected 54 active galaxies, 27 per each redshift bin. Note that six UHECR events lack any selected AGN counterpart located within 75 Mpc, and for two of them we also did not find any possible AGN association up to a distance 150 Mpc. Four of these are located at low Galactic latitudes,  $|b| < 12^\circ$ . Obviously, most of the events possess multiple AGN “counterparts” within the assumed search radius and redshift range.

We emphasize that the Véron-Cetty & Véron (2006) and NED assemblages are not complete AGN catalogs. Additionally, we have found several inconsistencies between these

<sup>9</sup> <http://nedwww.ipac.caltech.edu/>

TABLE 1. AGN POSSIBLY ASSOCIATED WITH UHECRS EVENTS

UHECR Event		AGN within 3.2° search radius			
Event number	Galactic Coordinates ( $\ell$ [°], $b$ [°])	0 < $z \leq 0.018$		0.018 < $z \leq 0.037$	
		Name	$\theta$ [']	Name	$\theta$ [']
25	(−21.8, 54.1)	NGC 5506	38	UM 653	136
				UM 654	138
				UM 625	171
18	(−57.2, 41.8)			ESO 575-IG016	55
				<b>MCG-03-32-017</b>	191
26	(−65.1, 34.5)			TOLOLO 00020	133
2	(−50.8, 27.6)	<b>NGC 5140</b>	116	<b>2MASX J13230241-3452464</b>	55
				<b>TOLOLO 00081</b>	95
				<b>ESO 444-G018</b>	144
21	(−109.4, 23.8)	<b>NGC 2907</b>	94		
		NGC 2989	182		
20	(−51.4, 19.2)	NGC 5128 (Cen A)*	54		
17	(−51.2, 17.2)	NGC 5128 (Cen A)*	139		
		<b>NGC 5064*</b>	162		
		NGC 5244	164		
8	(−52.8, 14.1)	<b>NGC 5064*</b>	47		
		<b>IRAS 13028-4909</b>	118		
		NGC 4945	121		
5	(−34.4, 13.0)	IC 4518A	66		
1	(15.4, 8.4)			<b>1RXS J174155.3-121157</b>	106
				HB91 1739-126	122
14	(−52.3, 7.3)			WKK 2031	83
23	(−41.7, 5.9)	<b>WKK 4374</b>	167		
3	(−49.6, 1.7)	DZOA 4653-11	40		
		<b>PKS 1343-60 (Cen B)</b>	41		
27	(−125.2, −7.7)				
11	(−103.7, −10.3)				
13	(−27.6, −16.5)	ESO 139-G012*	109		
		<b>AM 1754-634 NED03*</b>	191		
4	(−27.7, −17.0)	ESO 139-G012*	139		
		<b>AM 1754-634 NED03*</b>	166		
10	(48.8, −28.7)	CGCG 374-029	183	PC 2055+0126	125
				<b>Mrk 510</b>	152
19	(63.5, −40.2)	PC 2207+0122*	98	PKS 2201+044	109
				<b>NGC 7189*</b>	151
7	(58.8, −42.4)	PC 2207+0122*	189	<b>NGC 7189*</b>	108
16	(−170.6, −45.7)	NGC 1358*	51	Mrk 612	81
		NGC 1346*	66	Mrk 609*	133
		NGC 1320	130	<b>KUG 0322-063A*</b>	137
12	(−165.9, −46.9)	NGC 1346*	152	Mrk 609*	169
		NGC 1358*	166	<b>KUG 0322-063A*</b>	171
15	(88.8, −47.1)	<b>NGC 7626</b>	86	<b>2MASX J23274259+0845298</b>	122
		NGC 7591	186	NGC 7674	125
24	(12.1, −49.0)	NGC 7130	117	6dF J2132022-334254	127
		NGC 7135	126		
22	(−163.8, −54.4)	NGC 1204	96	MCG-02-08-039	174
9	(4.2, −54.9)	IC 5169	131	ESO 404-IG042	76
				PKS 2158-380	126
6	(−75.6, −78.6)	NGC 0424	25	ESO 351-G025	153
				<b>ESO 352-G048</b>	163

NOTE. —  $\theta$  denotes the separation between an UHECR event and an AGN. Stars denote AGN falling within the 3.2° search radius of two different events. AGN marked with bold font are those which *do not* appear in the Véron-Cetty & Véron (2006) catalog.

two databases regarding source classifications. This results in a few sources showing some (weak) level of AGN activity (according to one but not the other catalog) which might fulfill the criteria for a possible association with the detected UHECR events, but these are not included in our dataset<sup>10</sup>. However, a few other objects which do not obviously possess an active nucleus (but rather only H II central activity, like NGC 4945, NGC 5244, NGC 2989, NGC 7135, and espe-

cially nearby IRAS 13028-49<sup>11</sup>) are included and classified as “possibly LINERs.” Furthermore, the regions around 3 events (#7, #12, #16) are covered in the Sloan Digital Sky Survey (SDSS; York et al. 2000) leading to a somewhat misleading higher density of known AGN in these regions in comparison to other event regions. We have therefore omitted the 12 SDSS AGN in the Véron-Cetty & Véron (2006) list falling within the search volume from Tables 1, 2 and listed them separately in Table 3. These objects, all classified as Seyferts, are all located at redshifts  $z > 0.018$  and display similar bulk properties to the Seyferts we have included in our discussion. Most of the selected objects (50 out of 54) are relatively weak

<sup>10</sup> For example, we did not include the object ESO 383-G18 in our dataset, since its more accurate position from 2MASS as given in NED makes it 192.2' away from the location of CR#2. With the less accurate position listed by Véron-Cetty & Véron (2006), however, this source is <192' from the considered CR event.

<sup>11</sup> See Strauss et al. (1992).

TABLE 2. PROPERTIES OF SELECTED AGN

Name	Type	RA (J2000.0)	DEC (J2000.0)	$z$	$d_L$ [Mpc]	UHECR ( $\ell$ [°], $b$ [°])	$\theta$ [']	$S_R$ [mJy]	Ref.	$S_{FIR}$ [Jy]	$S_X$ [cgs]	Ref.
(1)	(2)	(3)	(4)	(5)	(6)	(7)	(8)	(9)	(10)	(11)	(12)	(13)
NGC 5506	Sy2	14h13m14.8s	−03d12m27s	0.0062	29	(−21.8, 54.1)	38	227	G06	8.4	12	S06
UM 653	Sy2	14h16m15.5s	−01d27m53s	0.0365	158	(−21.8, 54.1)	136	0.9 <sup>c</sup>	B95	0.4	—	—
UM 654	Sy2	14h16m19.7s	−01d25m18s	0.0369	160	(−21.8, 54.1)	138	<0.2 <sup>c</sup>	B95	—	—	—
UM 625	Sy2	14h00m40.6s	−01d55m18s	0.0250	109	(−21.8, 54.1)	171	1.1 <sup>c</sup>	B95	0.3	—	—
ESO 575-IG016	S2	12h52m36.2s	−21d54m46s	0.0229	100	(−57.2, 41.8)	55	1.7 <sup>c</sup>	C98	—	—	—
MCG-03-32-017	L(?)	12h38m00.5s	−20d07m51s	0.0280	123	(−57.2, 41.8)	191	<0.8 <sup>c</sup>	C98	—	—	—
TOLOLO 20	Sy1	12h12m20.0s	−28d48m46s	0.0300	131	(−65.1, 34.5)	133	<0.5 <sup>c</sup>	C98	—	—	—
2MASX J1323	L(?)	13h23m02.4s	−34d52m47s	0.0261	113	(−50.8, 27.6)	55	10.8 <sup>c</sup>	C98	—	—	—
TOLOLO 81	Sy2	13h19m38.6s	−33d22m54s	0.0291	127	(−50.8, 27.6)	95	<0.8 <sup>c</sup>	C98	—	—	—
NGC 5140	L(?)	13h26m21.7s	−33d52m06s	0.0129	58	(−50.8, 27.6)	116	29.2	S89	0.8	—	—
ESO 444-G018	L(?)	13h22m56.8s	−32d43m42s	0.0292	127	(−50.8, 27.6)	144	7.5 <sup>c</sup>	C98	—	—	—
NGC 2907	L(?)	09h31m36.7s	−16d44m05s	0.0070	33	(−109.4, 23.8)	94	4.4 <sup>c</sup>	M92	0.4	—	—
NGC 2989	L(?)	09h45m25.2s	−18d22m26s	0.0138	62	(−109.4, 23.8)	182	7.6 <sup>c</sup>	C98	1.7	—	—
NGC 5128 (Cen A)	FR I	13h25m27.6s	−43d01m09s	0.0018	3.4	(−51.4, 19.2)	54	53792	G94	162	30	B06
						(−51.2, 17.2)	139					
NGC 5064	L	13h18m59.9s	−47d54m31s	0.0099	45	(−51.2, 17.2)	162	4.0 <sup>c</sup>	M03	3.3	—	—
						(−52.8, 14.1)	47					
NGC 5244	L(?)	13h38m41.7s	−45d51m21s	0.0085	38	(−51.2, 17.2)	164	5.7 <sup>c</sup>	M03	1.9	—	—
IRAS 13028-49	Sy(?)	13h05m45.5s	−49d25m22s	0.0012	8.3	(−52.8, 14.1)	118	<22 <sup>c</sup>	B99	6.1	—	—
NGC 4945	Sy(?)	13h05m27.5s	−49d28m06s	0.0019	3.8	(−52.8, 14.1)	121	2953	G94	359	0.5	L04
IC 4518A	S2	14h57m41.2s	−43d07m56s	0.0163	70	(−34.4, 13.0)	66	64.9 <sup>c</sup>	M03	—	1.9 <sup>h</sup>	B07
IRXSS J174155	Sy1	17h41m55.3s	−12d11m57s	0.0370	156	(15.4, 8.4)	106	1.4 <sup>c</sup>	C98	—	2.9 <sup>h</sup>	B07
HB91 1739-126	Sy1	17h41m48.7s	−12d41m01s	0.0370	156	(15.4, 8.4)	122	<0.5 <sup>c</sup>	C98	—	—	—
WKK 2031	S2	13h15m06.3s	−55d09m23s	0.0308	133	(−52.3, 7.3)	83	154	G94	41.0	—	—
WKK 4374	Sy2	14h51m33.1s	−55d40m38s	0.0180	77	(−41.7, 5.9)	167	6.2 <sup>c</sup>	B99	—	2.0 <sup>h</sup>	B07
DZOA 4653-11	Sy1	13h47m36.0s	−60d37m04s	0.0129	56	(−49.6, 1.7)	40	<3.8 <sup>c</sup>	B99	—	7.8 <sup>h</sup>	B07
PKS 1343-60 (Cen B)	FR I	13h46m49.0s	−60d24m29s	0.0129	56	(−49.6, 1.7)	41	27100	W90	—	0.2 <sup>l</sup>	M05
ESO 139-G012	Sy2	17h37m39.1s	−59d56m27s	0.0170	71	(−27.6, −16.6)	109	5.2 <sup>c</sup>	M03	0.7	—	—
						(−27.7, −17.0)	139					
AM 1754-634	Sy(?)	18h00m10.9s	−63d43m34s	0.0157	65	(−27.6, −16.5)	191	<0.9 <sup>c</sup>	B99	—	—	—
						(−27.7, −17.0)	166					
PC 2055+0126	S(?)	20h58m18.2s	+01d38m00s	0.0260	105	(48.8, −28.7)	125	<0.8 <sup>c</sup>	C98	—	—	—
Mrk 510	Sy(?)	21h09m23.0s	−01d50m17s	0.0195	77	(48.8, −28.7)	152	48.4 <sup>c</sup>	W92	—	—	—
CGCG 374-029	S1	20h55m22.3s	+02d21m16s	0.0136	52	(48.8, −28.7)	183	1.8 <sup>c</sup>	C98	—	—	—
PC 2207+0122	S(?)	22h10m30.0s	+01d37m10s	0.0130	49	(63.5, −40.2)	98	<0.2 <sup>c</sup>	B95	—	—	—
						(58.8, −42.4)	189					
PKS 2201+044	BL	22h04m17.6s	+04d40m02s	0.0270	108	(63.5, −40.2)	109	530	W90	—	0.2 <sup>l</sup>	B94
NGC 7189	L	22h03m16.0s	+00d34m16s	0.0302	122	(63.5, −40.2)	151	13.0 <sup>c</sup>	C02	3.1	—	—
						(58.8, −42.4)	108					
NGC 1358	Sy2	03h33m39.7s	−05d05m22s	0.0134	54	(−170.6, −45.7)	51	8.7 <sup>c</sup>	C98	0.4	0.04	U05
						(−165.9, −46.9)	166					
Mrk 612	Sy2	03h30m40.9s	−03d08m16s	0.0205	83	(−170.6, −45.7)	81	5.1 <sup>c</sup>	C98	1.2	0.04	G05
NGC 1320	Sy2	03h24m48.7s	−03d02m32s	0.0089	35	(−170.6, −45.7)	130	3.3	G06	2.2	—	—
Mrk 609	Sy2	03h25m25.3s	−06d08m38s	0.0345	143	(−170.6, −45.7)	133	12.5 <sup>c</sup>	C98	2.6	—	—
						(−165.9, −46.9)	169					
KUG 0322-063	Sy1	03h25m11.6s	−06d10m51s	0.0338	140	(−170.6, −45.7)	137	11.3 <sup>c</sup>	C98	2.1	—	—
						(−165.9, −46.9)	171					
NGC 1346	L(?)	03h30m13.3s	−05d32m36s	0.0135	54	(−170.6, −45.7)	66	10.4 <sup>c</sup>	C98	3.1	—	—
						(−165.9, −46.9)	152					
NGC 7626	L	23h20m42.5s	+08d13m01s	0.0114	42	(88.8, −47.1)	86	210	W90	—	0.03 <sup>l</sup>	T05
2MASX J2327	Sy2	23h27m42.6s	+08d45m30s	0.0294	118	(88.8, −47.1)	122	<0.5 <sup>c</sup>	C98	—	—	—
NGC 7674	Sy2	23h27m56.7s	+08d46m45s	0.0289	116	(88.8, −47.1)	125	90.6 <sup>c</sup>	C02	5.6	0.05	L04
NGC 7591	L	23h18m16.3s	+06d35m09s	0.0165	64	(88.8, −47.1)	186	21.4 <sup>c</sup>	C02	7.2	—	—
NGC 7130	Sy2	21h48m19.5s	−34d57m05s	0.0161	64	(12.1, −49.0)	117	63.3 <sup>c</sup>	M03	16	0.006	Gm06
NGC 7135	L(?)	21h49m46.0s	−34d52m35s	0.0088	33	(12.1, −49.0)	126	2.3 <sup>c</sup>	C98	0.2	—	—
6dF J2132022	Sy1	21h32m02.2s	−33d42m54s	0.0293	120	(12.1, −49.0)	127	1.1 <sup>c</sup>	C98	—	—	—
NGC 1204	L	03h04m39.9s	−12d20m29s	0.0143	57	(−163.8, −54.4)	96	9.4 <sup>c</sup>	C90	7.8	—	—
MCG-02-08-039	Sy2	03h00m30.6s	−11d24m57s	0.0299	123	(−163.8, −54.4)	174	3.6 <sup>c</sup>	C98	0.5	—	—
ESO 404-IG042	S2	22h13m17.5s	−37d00m58s	0.0340	140	(4.2, −54.9)	76	2.2 <sup>c</sup>	C98	0.7	—	—
PKS 2158-380	FR II	22h01m17.1s	−37d46m24s	0.0333	137	(4.2, −54.9)	126	590	W90	0.3	—	—
IC 5169	Sy2	22h10m10.0s	−36d05m19s	0.0104	39	(4.2, −54.9)	131	8.3 <sup>c</sup>	M03	3.4	—	—
NGC 0424	Sy1	01h11m27.6s	−38d05m00s	0.0118	46	(−75.6, −78.6)	25	9.6 <sup>c</sup>	C98	1.8	0.1	U05
ESO 351-G025	Sy2	00h58m22.3s	−36d39m37s	0.0346	143	(−75.6, −78.6)	153	2.4 <sup>c</sup>	C98	—	—	—
ESO 352-G048	Sy2	01h20m54.7s	−36d19m26s	0.0322	132	(−75.6, −78.6)	163	<0.5 <sup>c</sup>	C98	—	—	—

REFERENCES. — (B95) Becker et al. 1995; (B06) Beckmann et al. 2006; (B07) Bird et al. 2007; (B99) Bock et al. 1999; (B94) Brinkmann et al. 1994; (C90) Condon et al. 1990; (C98) Condon et al. 1998; (C02) Condon et al. 2002; (G06) Gallimore et al. 2006; (Gm06) González-Martín et al. 2006; (G94) Gregory et al. 1994; (G05) Guainazzi et al. 2005; (L04) Lutz et al. 2004; (M05) Marshall et al. 2005; (M03) Mauch et al. 2003; (M92) Mollenhoff et al. 1992; (S89) Sadler et al. 1989; (S06) Shinozaki et al. 2006; (T05) Tajer et al. 2005; (U05) Ueda et al. 2005; (W92) White & Becker 1992; (W90) Wright & Otrupcek 1990.

NOTE. — [1] Name of the source. [2] AGN classification (the Sy1/Sy2: Seyfert galaxy of the type 1/type 2; L: LINER; FR I: radio galaxy of the FR I type; BL: BL Lacertae object). [3-4] Equatorial coordinates (J2000.0). [5] Redshift of the source. [6] Luminosity distance for the assumed cosmology ( $H_0 = 73 \text{ km s}^{-1} \text{ Mpc}^{-1}$ ,  $\Omega_M = 0.27$ ,  $\Omega_\Lambda = 0.73$ ) except for NGC 5128 (Cen A) and NGC 4945, where the distances are known (Karachentsev et al. 2007). [7] Galactic coordinates for the nearby UHECR event. [8] Separation between an AGN and a nearby UHECR event. [9] The total 5 GHz flux in mJy units (<sup>c</sup> fluxes converted from the ones provided at lower frequencies assuming radio spectral index  $\alpha = 0.7$ ). [10] References for column 9. [11] The total 60  $\mu\text{m}$  flux in Jy units from the IRAS survey (Moshir et al. 1990). [12] The total observed  $2 - 10 \text{ keV}$  flux in  $\times 10^{-11} \text{ erg cm}^{-2} \text{ s}^{-1}$  units (<sup>h</sup> fluxes provided at lower photon energy range:  $0.5 - 7 \text{ keV}$  in Marshall et al. (2005), or  $0.1 - 2.0 \text{ keV}$  in Brinkmann et al. (1994) and Tajer et al. (2005); <sup>h</sup> fluxes converted from the ones provided at higher photon energy range  $40 - 100 \text{ keV}$  in Bird et al. (2007), assuming X-ray photon index  $\Gamma_X = 2.0$ ). [13] References for column 12.

TABLE 3. SDSS AGN (HAO ET AL. 2005).

Event Number	Name	Type	$z$	$\theta$ [']
(1)	(2)	(3)	(4)	(5)
7	SDSS J215259.07-000903.4	Sy2	0.028	188
	SDSS J220515.43-010733.3	Sy2	0.032	7
12	SDSS J033458.00-054853.2	Sy1	0.018	123
	SDSS J034545.16-071526.8	Sy2	0.022	172
	SDSS J033955.97-063228.9	Sy2	0.031	113
	SDSS J033713.31-071718.0	Sy2	0.033	53
	SDSS J032329.63-062944.1	Sy2	0.034	182
	SDSS J034330.25-073507.4	Sy2	0.036	135
16	SDSS J033458.00-054853.2	Sy1	0.018	97
	SDSS J033955.97-063228.9	Sy2	0.031	179
	SDSS J033713.31-071718.0	Sy2	0.033	190
	SDSS J032329.63-062944.1	Sy2	0.034	168

NOTE. — [1] UHECR Event Number. [2] Name of the source (note that source positions are implicit in the SDSS names). [3] AGN classification (Sy1/Sy2: Seyfert galaxy of the type 1/type 2). [4] Redshift of the source. [5] Separation between an AGN and a nearby UHECR event.

Seyfert galaxies and LINERs, while only a small fraction (4) are bright and well established jet sources (three radio galaxies and one BL Lac object).

It is probable that more Seyferts/LINERs are missing (as evident in the SDSS covered regions) and/or mis-classified in the presented AGN collection. However, we expect much fewer radio galaxies/BL Lacs to be omitted. For an order of magnitude estimate, we derive an average number density of radio galaxies within the redshift range  $z \leq 0.037$  of  $\sim 3 \times 10^{-6} \text{ Mpc}^{-3}$  (consistent with an estimate of the space density of UHECR sources given below) assuming the total radio luminosity range between  $10^{38} \text{ erg s}^{-1}$  and  $\geq 10^{42} \text{ erg s}^{-1}$ . This was derived using the 151 MHz luminosity function of low-power radio sources (including classical FR I, and FR II radio galaxies with weak/absent emission lines) of Willott et al. (2001), converting their model C to the modern cosmology adopted in this paper (discussed in detail in Stawarz et al. 2006) and the total 151 MHz luminosities to 5 GHz ones assuming a radio spectral index of  $\alpha_R = 0.7$ . The derived number density of local radio galaxies is therefore about three orders of magnitude lower than the number density of Seyfert galaxies (see below), resulting in a total of  $\sim 42$  expected radio galaxies within the co-moving volume of the local Universe  $V = 0.014 \text{ Gpc}^3$ . We note that with the assumed minimum radio luminosity one order of magnitude lower, i.e.  $10^{37} \text{ erg s}^{-1}$ , the number density of radio galaxies increases by a factor of  $\sim 4$ . At such low radio luminosities, however, the luminosity function constructed by Willott et al. (2001) is not well determined.

With the small number of nearby radio galaxies, we expect that the majority of these objects have already been identified as such through radio imaging studies. The luminosities of the radio galaxies/BL Lac in our sample (down to  $4 \times 10^{39} \text{ erg s}^{-1}$ , the 5 GHz luminosity of Cen A), correspond to a relatively bright flux limit ( $\sim 100 \text{ mJy source}^{12}$  at  $D = 160 \text{ Mpc}$ ). The morphologies of such bright radio sources have been well surveyed (e.g., Owen et al. 1995; Sadler et al. 1989, and references therein) although admittedly, there is sparser coverage in some parts of the sky, in, e.g., the Southern hemisphere (Burgess & Hunstead 2006). The Galactic plane is particu-

larly susceptible to having unidentified local radio galaxies but the radio imaging surveys toward the plane are maturing (Helfand et al. 2006) and hard X-ray surveys are beginning to help rectify the situation (e.g., Molina et al. 2007).

Table 2 lists the main properties of all the selected AGN collected from the literature, in particular the total radio fluxes at 5 GHz (or upper limits for these), *IRAS* fluxes at  $60 \mu\text{m}$  (if available), and 2 – 10 keV fluxes (again, if available). In some cases, the flux conversion from values provided at lower radio frequencies (or in higher X-ray photon energy range) was necessary, and we performed this assuming typical values of the radio spectral index  $\alpha_R = 0.7$  (X-ray photon index  $\Gamma_X = 2.0$ ). Note that 12 sources listed in Table 2 have only upper limits for the total radio emission which were derived by us from the *FIRST* (Becker et al. 1995), *NVSS* (Condon et al. 1998), or *SUMMS* (Bock et al. 1999) surveys, and most of them are indeed very weak radio sources ( $< \text{mJy level}$ ).

Only in the case of the four selected FR I/BL Lac sources (Cen A, Cen B, PKS 2158–380, PKS 2201+044) is the presence of relativistic jets – as ones considered in different models for the acceleration of UHECRs – certain. As for the rest of the selected AGN, one should ask if jet activity can be ascertained and, if so, what are the properties of the jets in these sources. Are these jets relativistic? What are their inclinations? Do they differ somehow from the jets observed in other Seyfert and LINER galaxies? Such questions are relevant, because the space density of the local low-luminosity AGN, just like the ones selected in our sample, is high. For example, the space density of bright galaxies ( $-22 \text{ mag} \leq M_B \leq -18 \text{ mag}$ ) showing Seyfert activity is  $\sim 1.25 \times 10^{-3} \text{ Mpc}^{-3}$  (Ulvestad & Ho 2001)<sup>13</sup> which is  $\sim 10 - 10^3$  times larger than the space density of UHECR sources,  $\sim 10^{-6} - 10^{-4} \text{ Mpc}^{-3}$ , derived from a comparison of simulation of particle propagation in the local universe and the Akeno Giant Air Shower Array (AGASA) data (Blasi & De Marco 2004; Sigl et al. 2004; Takami et al. 2006). Note that Dubovsky et al. (2000) gives an estimate of the space density of UHECR sources  $\sim 6 \times 10^{-3} \text{ Mpc}^{-3}$  based on 7 observed doublets (only two events have estimated energy  $> 100 \text{ EeV}$ ) and assuming the distance  $\lesssim 25 \text{ Mpc}$  for protons  $> 100 \text{ EeV}$ . When rescaled to the distance  $\lesssim 75 \text{ Mpc}$ , it gives  $\sim 2 \times 10^{-4} \text{ Mpc}^{-3}$ , consistent with other estimates. Recently Takami & Sato (2008) estimated a space density of UHECR sources  $\sim 10^{-4} \text{ Mpc}^{-3}$  based on the Auger data. Thus, restricting the investigations to redshifts  $z \leq 0.037$ , corresponding to the luminosity distance  $d_L \leq 156.4 \text{ Mpc}$  and co-moving volume  $V = 0.014 \text{ Gpc}^3$ , there are  $\sim 1.8 \times 10^4$  low-luminosity AGN with surface density (if distributed isotropically over the whole sky)  $\sim 1.4 \times 10^3$  per steradian. In other words, there should be  $\sim 14$  AGN within the search radius  $3.2^\circ$ . The much lower rate of our possible identification given in Table 1 is due to incompleteness/lack of the AGN surveys in different parts of the sky, and especially within the Galactic Plane (see a decrease in the identification rate for Galactic latitudes  $|b| < 12^\circ$  in Table 1). Therefore, if the selected Seyferts and LINERs do not differ from the other local AGN of the same types, the claimed correlation between the UHECR events and local active galaxies should be considered as rather unlikely, resulting from a chance coincidence, if the production of the highest

<sup>13</sup> This is about  $\sim 10^3$  times larger than the local space density of bright quasars, and  $\sim 10$  times smaller than the space density of “regular” galaxies with comparable brightness (Ulvestad & Ho 2001).

<sup>12</sup> For  $\alpha_R = 0.7$ , this corresponds to  $\sim 250 \text{ mJy}$  at 1.4 GHz.



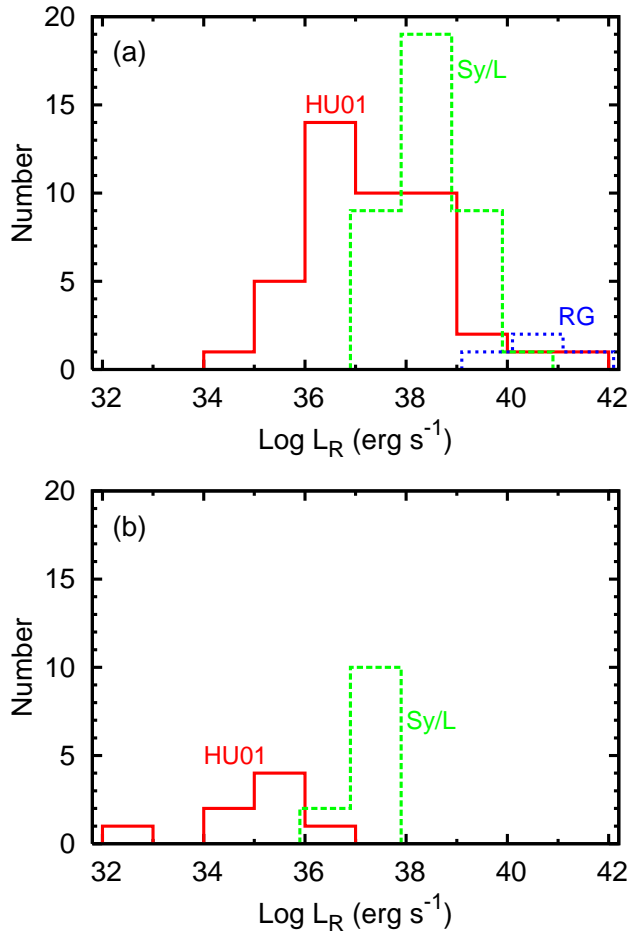


FIG. 1.— (a) Number distributions of 5 GHz total radio powers for Seyfert galaxies detected at radio frequencies from the sample constructed by Ho & Ulvestad (2001, red solid), Seyfert/LINER galaxies from our sample detected at radio frequencies (green dashed), and radio galaxies from our sample (blue dotted). (b) Number distributions of upper limits to 5 GHz total radio powers for Seyfert galaxies detected at radio frequencies from the sample constructed by Ho & Ulvestad (2001, red solid), and Seyfert/LINER galaxies from our sample detected at radio frequencies (green dashed). The histograms are slightly shifted relative to each other in horizontal direction for clarity.

energy CRs is not episodic in nature, but operates in a single object on long ( $\geq$  Myr) timescales. In addition, if the selected sources do not show significant jet activity, there are no reasons for expecting them to accelerate CRs up to 10–100 EeV energies.

A brief summary of the radio properties of local low-luminosity AGN given in §2 allows us to conclude that the particular Seyferts and LINERs selected in Table 2 are most likely jetted, but do not differ from the other analogous sources of the same type. In particular, complex radio morphologies consisting of compact cores, one-sided jets, and extended halos, as found in several of the selected objects, are typical for the Seyfert/LINER-type jet activity (see §2). Such jets are expected to be sub-relativistic ( $v < 0.25c$  on pc-scales), low-power ( $L_j \leq 10^{43}$  erg s $^{-1}$ ), precessing and short-lived ( $t_j \lesssim 10^5$  yrs). Indeed, 5 GHz powers for the selected Seyferts and LINERs, being in a range  $L_{5\text{ GHz}} \sim 10^{37} - 10^{42}$  erg s $^{-1}$ , are typical for the other AGN of the same kind,

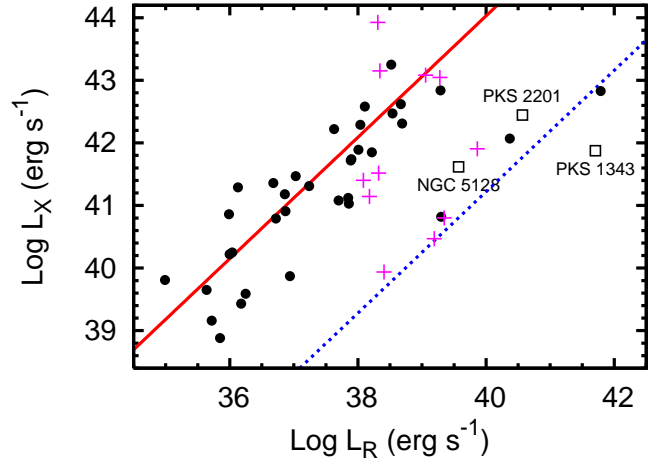


FIG. 2.— X-ray (2 – 10 keV) luminosity versus 5 GHz total luminosity for Seyfert galaxies from the sample constructed by Panessa et al. (2007, black circles), Seyfert/LINER galaxies from our sample with the X-ray and 5 GHz fluxes provided (magenta crosses), radio galaxies from our sample with the X-ray fluxes provided (open squares). In the case of the sample of Panessa et al. (2007), only sources detected at X-ray and radio frequencies were considered. Red solid line indicates the best fit  $\log L_X = 0.97 \log L_R + 5.23$  for Seyfert galaxies, and blue dotted line denotes the best fit  $\log L_X = 0.97 \log L_R + 2.42$  for low-luminosity radio galaxies, both as given by Panessa et al.

and are significantly lower than the radio powers of 4 selected radio galaxies/BL Lac. The median values of these,  $\sim 2 \times 10^{38}$  erg s $^{-1}$  (including only radio-detected sources), seems to be higher than the appropriate median values given by Ho (2008), but this may be simply due to selection effects. In fact, all 12 objects for which only upper limit regarding the radio fluxes are provided, have  $L_{5\text{ GHz}} < 5 \times 10^{37}$  erg s $^{-1}$ .

Figure 1a shows the number distributions of 5 GHz total radio powers for Seyfert galaxies detected at radio frequencies from the optically selected sample constructed by Ho & Ulvestad (2001), the Seyfert/LINER galaxies from our sample detected at radio frequencies, and radio galaxies from our sample. At first glance, our Seyferts/LINERs appear systematically more radio luminous in comparison to the Ho & Ulvestad (2001) sample by 1–2 dex. However, we note that the upper limits we obtain from the available “all-sky” maps (NVSS, SUMMS) are systematically higher than the ones obtained by Ho & Ulvestad from their pointed observations (Figure 1b) also by 1–2 orders of magnitude, making it difficult to compare the two distributions directly. The radio galaxies are characterized by larger radio luminosities than Seyferts/LINERs, as expected.

The range of X-ray luminosities (if available) of objects in our sample is in the range  $L_{2-10\text{ keV}} \sim 10^{40} - 10^{44}$  erg s $^{-1}$  (with the median  $\sim 3 \times 10^{41}$  erg s $^{-1}$  again slightly higher than the one provided by Ho 2008), which is comparable to the typical 2–10 keV luminosities observed in local low-power AGN (Panessa et al. 2007). Moreover, the logarithm of the ratio of the X-ray and radio luminosities,  $\log(L_{5\text{ GHz}}/L_{2-10\text{ keV}})$ , although widely scattered in a range between (–1.3) and (–5.6) with median (–3.2), is in agreement with the values found in other local low-luminosity AGN (see Panessa et al. 2007).

Figure 2 shows the X-ray (2 – 10 keV) luminosity versus 5 GHz total luminosity for Seyfert galaxies from the sample constructed by Panessa et al. (2007), Seyfert/LINER galaxies from our sample with the X-ray and 5 GHz fluxes provided,



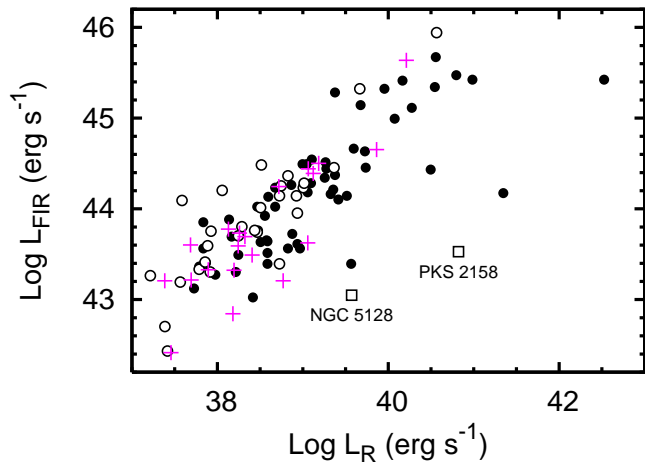


FIG. 3.—  $60\ \mu\text{m}$  luminosity versus 5 GHz total luminosity for Seyfert galaxies from the sample constructed by Roy et al. (1998, detections: *black circles*, upper limits: *open circles*), Seyfert/LINER galaxies from our sample with the  $60\ \mu\text{m}$  and 5 GHz fluxes provided (*magenta crosses*), radio galaxies from our sample with the  $60\ \mu\text{m}$  fluxes provided (*open squares*). In the case of the sample of Roy et al. (1998), sources classified as quasars were omitted, and radio luminosities provided at 2.4 GHz were converted to 5 GHz luminosities assuming radio spectral index  $\alpha_R = 0.7$ .

and radio galaxies from our sample with the X-ray fluxes provided. In the case of the sample of Panessa et al. (2007), only sources detected at X-ray and radio frequencies were considered. The bulk of our selected Seyferts/LINERs match well the  $L_X - L_R$  correlation established for nearby Seyferts. Our selected radio galaxies and a few Seyferts are over-luminous in the radio for a given X-ray luminosity when compared to the Seyferts. However, they match well the  $L_X - L_R$  correlation established for nearby “low-luminosity radio galaxies” (LLRGs, Panessa et al. 2007).

Finally, the ratio of FIR and radio luminosities for the selected Seyferts and LINERs agrees with what is observed in other analogous sources. Namely, the median value in our sample is  $\log(L_{60\ \mu\text{m}}/L_{5\ \text{GHz}}) \sim 5.37$  for Seyferts and LINERs. These can be compared with the medians claimed by Ho & Ulvestad (2001) for Seyferts,  $\sim 5.31$ , and for regular spiral galaxies,  $\sim 5.64$ , implying that the Seyferts and LINERs included in our sample are not more than twice brighter in radio than expected if all the radio emission is due to star-forming activity, in agreement with the established properties of other Seyferts. We note that the analogous ratios for the two radio galaxies included in the sample and detected at FIR are significantly lower,  $\log(L_{60\ \mu\text{m}}/L_{5\ \text{GHz}}) \sim 2.8$  and  $3.5$ , as expected.

Figure 3 shows the  $60\ \mu\text{m}$  luminosity versus 5 GHz total luminosity for Seyfert galaxies from the sample constructed by Roy et al. (1998), Seyfert/LINER galaxies from our sample with the  $60\ \mu\text{m}$  and 5 GHz fluxes provided, and radio galaxies from our sample with the  $60\ \mu\text{m}$  fluxes provided. In the case of the sample of Roy et al. (1998), sources classified as quasars were omitted, and radio luminosities provided at 2.4 GHz were converted to 5 GHz luminosities assuming a radio spectral index  $\alpha_R = 0.7$ . All our selected Seyferts/LINERs match the FIR–radio correlation established for other nearby Seyferts. Our selected radio galaxies are over-luminous in radio for a given FIR luminosity with respect to Seyferts, as expected.

### 3.1. Selected radio galaxies

As already discussed in §2, radio activity in low-power active galaxies of the Seyfert or LINER type differ substantially from that observed in well established jet sources like radio galaxies and radio-loud quasars. Indeed, there are some important reasons for such a difference. In particular, Seyferts and LINERs are usually hosted by spiral (disk) galaxies, while radio galaxies and radio-loud quasars are typically hosted by giant ellipticals. It was noted recently that merger episodes triggering jet activity (by shaping the accretion processes and even determining spins of supermassive black holes), proceed differently depending on the host properties (Hopkins & Hernquist 2006; Sikora et al. 2007; Volonteri et al. 2007).

Of the 54 selected AGN (Table 2), 3 are classified as radio galaxies and one is a BL Lac object, i.e., under the unification scheme, it is a FR I observed with a small jet viewing angle (Urry & Padovani 1995). This group includes Cen A (Figure 4), which is characterized by a well-known FR I radio morphology with a one-sided ( $\sim 4$  kpc long) jet and giant ( $\sim 0.5$  Mpc) radio lobes (e.g., Israel 1998). This is the only source in the sample detected in  $\gamma$ -rays (Sreekumar et al. 1999; Steinle et al. 1998). Radio maps of Cen B reveal a one-sided well-defined FR I jet extending from pc- to kpc-scales, and an edge-brightened structure on the opposite lobe more characteristic of a powerful FR II (Figure 5, Jones et al. 2001). From our new VLA map of PKS 2158–380 (Figure 6), its radio morphology is characteristic of a FR II with bright compact features at the outer edges of its lobes. It is, however, relatively underluminous for a FR II ( $L_{1.4\ \text{GHz}} \sim 4 \times 10^{24}\ \text{W Hz}^{-1}$ ) and can be considered an intermediate object. PKS 2201+044 is classified as a BL Lac object with an asymmetric core-jet radio structure (Figure 7), and an extended ( $\sim 100$  kpc) radio halo (Augusto et al. 1998). These four objects are quite representative of the local population of radio galaxies. Note that Cen A is exceptionally bright and extended in the sky only due to its proximity.

In fact, due to its large extent on the sky, Cen A may be considered as being likely associated with more than two Auger events (see Figure 4). Note that Table 1 indicates a possible association of Cen A with only two CR events, because the  $3.2^\circ$  separation of the UHECR event from the Cen A *nucleus* is assumed when compiling the list of the selected AGN). Considering the 9 events plotted in Figure 4 around the giant radio structure of Cen A, their detection rate appears steady (almost every third event detected by Auger, except for the larger gap between events #8 and #14). If the rate is indeed steady, as would be expected if giant Mpc-scale radio lobes of Cen A are the acceleration sites of these events, this will be easily tested with additional 2–4 years of Auger observations.

Considering the four events closest to Cen A, the positions of these four events are roughly aligned with the axis of the radio lobes, which is also aligned with the super-galactic plane (cf. Figure 2 of Abraham et al. 2008a). The latter two events are closest to the center of Cen A and the former two are coincident with other AGN in the field. It is of interest to note that one of the field AGN is NGC 4945 (event #8), which is located in the Centaurus group (i.e., it is at the same approximate distance as Cen A). NGC 4945 hosts a less powerful radio source than Cen A and is dominated by extended emission from the galaxy and a compact non-thermal core (Elmouttie et al. 1997). Also, of the 6 UHECR events without an associated nearby ( $z < 0.018$ ) AGN within a  $\theta \leq 3.2^\circ$  cir-

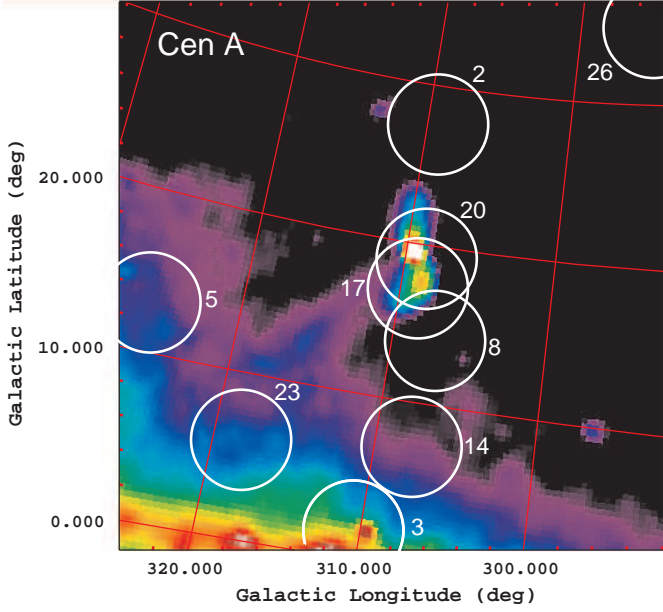


FIG. 4.— Radio map (at 408 MHz from Haslam et al. 1982) of the  $35^\circ \times 35^\circ$  field centered on the nearby radio galaxy Cen A. The total extent of the north-south radio lobes is  $\sim 9^\circ$  and is centered on the AGN (the bright white region near the center of the field). The  $r = 3.2^\circ$  circles mark the positions of the UHECR events detected in the field by Auger (Abraham et al. 2008a). The numbers correspond to the event number as provided in Abraham et al. (2008a), and also in our Table 1. Note event #3 corresponds most closely to Cen B, a bright spot near the center of the circle, shown with higher resolution in Figure 5.

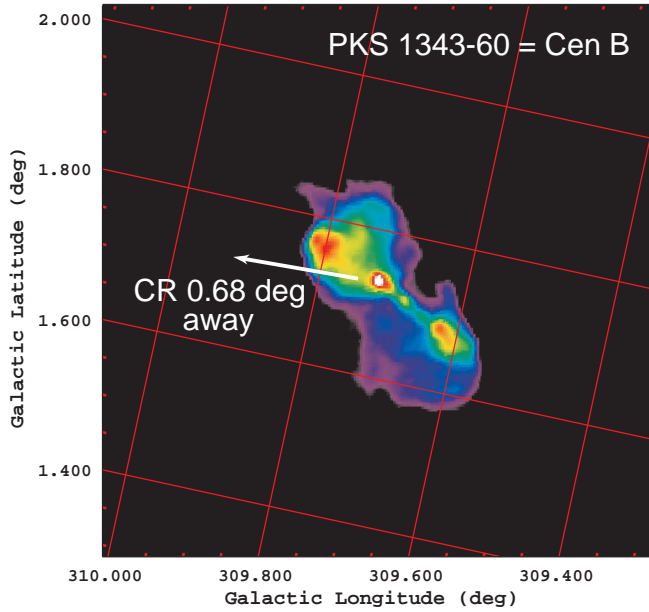


FIG. 5.— Radio image of the  $0.75^\circ \times 0.75^\circ$  field centered on the radio galaxy Cen B. The  $43''$  resolution image was obtained with the MOST at 843 MHz by McAdam (1991). The location of the closest CR detected by Auger (#3; c.f. Figure 4) is indicated by the arrow pointing away from the radio nucleus.

cular area, 2 are in the plotted field (#14, #26). However, #14 is the one closest to the Galactic Plane, where it is more difficult to identify AGN, and #26 is the one furthest from Cen A. As discussed in the next Section a larger deflection angle for the events close to the Galactic plane is possible, which could

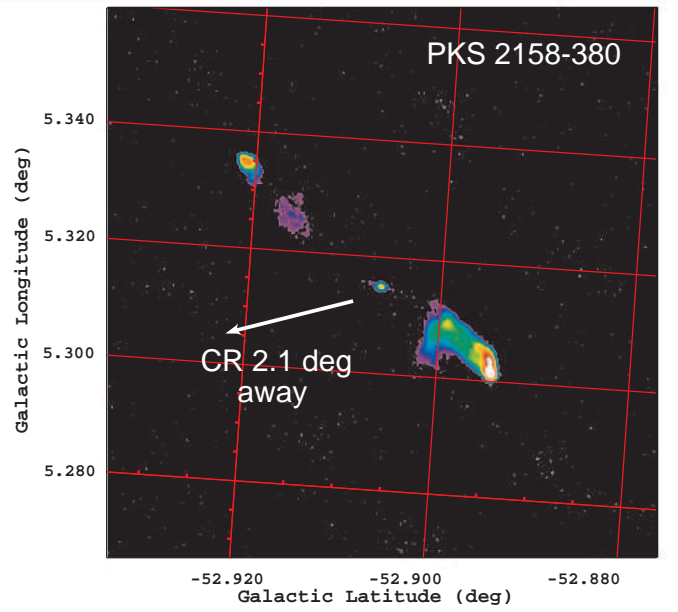


FIG. 6.— Radio image of the  $200'' \times 200''$  field around the radio galaxy PKS 2158–380. This VLA 4.9 GHz image at  $2''$  resolution was made using a multi-configuration dataset consisting of a 1 hr observation in Dec 1983 (program AT45) and 10 min observation from Jun 1997 (AK444). The latter dataset was obtained through the NRAO VLA Archive Survey (NVAS). The location of the closest cosmic ray detected by Auger (#9) is indicated by the arrow pointing away from the radio nucleus. (This NVAS image was produced as part of the NRAO VLA Archive Survey, (c) AUI/NRAO.)

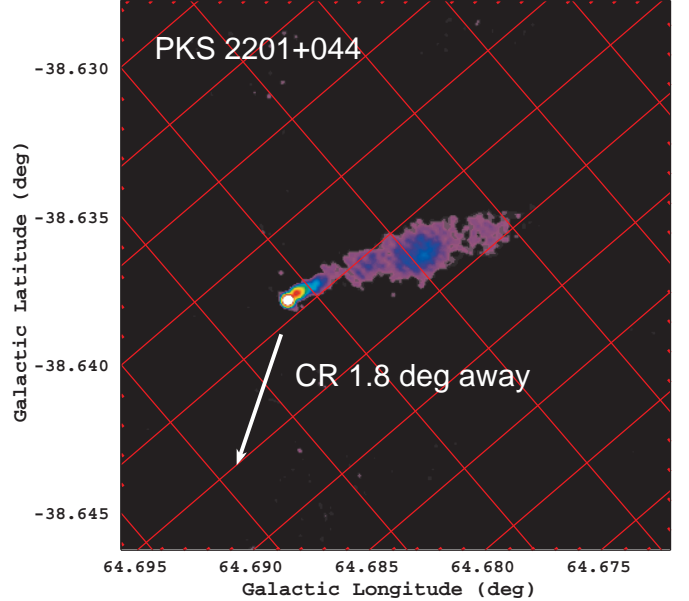


FIG. 7.— Radio image of the  $100'' \times 100''$  field around the BL Lac object PKS 2201+044 showing its one-sided radio jet. The image is a lower resolution ( $1''$  beam) version of the VLA 8.5 GHz data published in Sambruna et al. (2007). The location of the closest CR detected by Auger (#19) is indicated by the arrow pointing away from the radio nucleus.

mean that Cen B could be associated with more than 1 event.

#### 4. PROPAGATION AND COMPOSITION OF UHECRS

The propagation of the UHECRs from the sources to the observer is not rectilinear due to deflection by intervening mag-

netic fields. The magnetic field structure (both extragalactic and Galactic), along with the UHECR source distribution, the nature of sources (transient vs. steady), the energy spectrum at the injection, and the CR composition, are all “known unknown” factors that affect the distribution of the observed arrival directions.

Though quite an extensive literature on simulation of UHECR propagation in extragalactic magnetic fields exists, very little is known about the strength and configuration of such fields. So far, direct evidence for the presence of extragalactic magnetic fields has been found only in galaxy clusters (for a review see Carilli & Taylor 2002). Faraday rotation measurements provide evidence for intracluster core fields in the range of 1 – 10  $\mu\text{G}$ . Outside clusters only upper limits at the level 1 – 10 nG are available. Extragalactic magnetic fields are *ad hoc* assumed to have a domain structure with a Kolmogorov power spectrum and a uniform correlation length. Toy models assume a field strength  $\sim 1$  nG in voids with a somewhat larger field  $\sim 10$  nG at the supergalactic plane (e.g., Stanev et al. 2003).

Recent simulations of magnetic fields in the intergalactic medium are more sophisticated. They take into account the growth of the magnetic fields from seed fields such that the resulting field strength traces the baryon density as the large-scale structure evolves. A more realistic extragalactic magnetic field of this nature may result in significantly larger deflections than is expected from a purely random field. A simulation by Sigl et al. (2004) used the Biermann battery mechanism to generate seed fields which were evolved, and then rescaled so that the magnetic field in the core of a simulated Coma-like galaxy cluster is comparable to the  $\mu\text{G}$  fields as indicated by Faraday rotation measures. Simulations of large-scale structure formation and the build-up of magnetic fields in the intergalactic medium have also been performed by Dolag et al. (2005). The basic assumption is that cosmological magnetic fields grow in a magnetohydrodynamic amplification process driven by the formation of structure from a magnetic seed field present at high redshift. The initial density fluctuations were constructed from the IRAS 1.2-Jy galaxy survey by first smoothing the observed galaxy density field on a scale of 7 Mpc, evolving it linearly back in time and then using it as a Gaussian constraint for an otherwise random realization of a  $\Lambda\text{CDM}$  cosmology (Mathis et al. 2002). As a result, the positions and masses of prominent galaxy clusters coincide closely with their real counterparts in the local universe. Takami et al. (2006) have used a magnetic field strength scaled with the matter density  $|B| \propto \rho^{2/3}$ , where the distribution of galaxies is constructed using the IRAS PSCz catalog. The correlation length is taken to be 1 Mpc and the magnetic field is assumed to be represented as a Gaussian random field with a Kolmogorov power spectrum in each cube. The field is further renormalized to obtain  $\sim 0.4 \mu\text{G}$  in a cube that contains the center of the Virgo Cluster.

The average deflection angle in a random field is  $\langle \theta_d \rangle \approx 2.5^\circ Z E_{20}^{-1} B_{-9} (D_{100} l_1)^{1/2}$ , where  $Z$  is the particle charge,  $D_{100}$  is the distance in units 100 Mpc,  $B_{-9}$  is the r.m.s. field strength in nG,  $E_{20}$  is the particle energy in units  $10^{20}$  eV, and  $l_1$  is the correlation length in Mpc (e.g., Waxman & Miralda-Escudé 1996). The *average* time delay corresponding to the *average* deflection angle  $\langle \theta_d \rangle$  is  $\langle \tau \rangle \sim \langle \theta_d^2 \rangle D / 4c$  (Alcock & Hatchett 1978, their eq. [29]), where  $\langle \theta_d^2 \rangle = 4 \langle \theta_d \rangle^2 / \pi$  can be derived from  $\theta_d^2$  probability distribution (their eq. [23]), and  $c$  is the speed of light. This yields

$\langle \tau \rangle \sim \langle \theta_d \rangle^2 D / \pi c \sim 2 \times 10^5 Z^2 E_{20}^{-2} B_{-9}^2 D_{100}^2 l_1$  yr. For a  $10^{20}$  eV proton injected at  $D \sim 75$  Mpc for characteristic values of  $B_{-9} \sim 1$  and  $l_1 \sim 1$ ,  $\langle \theta_d \rangle \sim 2^\circ$  and  $\langle \tau \rangle \sim 1.6 \times 10^5$  yr which is comparable to the crossing time of the Galaxy and the characteristic timescale of jet lifetimes in Seyfert galaxies as discussed earlier, but is negligible compared to the galactic evolution timescale. Therefore, observations at different wavelengths show us *nearly* a snapshot of the sources at the time when the highest energy CRs were emitted. If a detected CR particle has been accelerated by a pc-scale jet, the jet will expand during the time delay to become larger,  $\sim 10^5$  lt-yr, and this may be seen as a more extended structure in the radio. The association of UHECR accelerators must correspondingly take into account such time delays and source evolution since observed photon signals come from later times than the epoch of UHECR escape from the source.

The Galactic magnetic field is known much better than the extragalactic one. It can be determined from pulsar rotation and dispersion measures combined with a model for the distribution of free electrons (e.g., Cordes & Lazio 2003a,b). A large-scale field of a few  $\mu\text{G}$  aligned with the spiral arms exists, but there is no general agreement on the details (Beck 2001). Recent studies give a bisymmetric model for the large-scale Galactic magnetic field with reversals on arm-interarm boundaries (Brown et al. 2007; Han 2008; Han et al. 2006). Independent estimates of the strength and distribution of the field can be made by simultaneous analysis of radio synchrotron, CR, and  $\gamma$ -ray data, and these confirm a value of a few  $\mu\text{G}$ , increasing towards the inner Galaxy (Strong et al. 2000, and Strong et al. *in prep.*). The magnetic field in the halo is less known. Observations of the rotation measure of extragalactic radio sources reveal azimuthal magnetic fields in the halo with reversed directions below and above the plane consistent with A0 symmetry type (Han 2008; Wiełebinski & Krause 1993).

Because of their large Larmor radii  $> 1$  kpc ( $r_L \approx 10^5 E_{20} / B_{-9}$  kpc), UHECRs propagating in the Galactic magnetic field are sensitive to the global topology of the field. The influence of the geometry of the Galactic magnetic field has been studied in various source distribution scenarios (Alvarez-Muñiz 2002; Stanev 1997; Takami et al. 2006). For a  $\sim 1 \mu\text{G}$  magnetic field, the distance  $D \sim 100$  kpc, and a correlation length  $l \sim 1$  kpc, the average deflection angle is  $\langle \theta_d \rangle \sim 2.5^\circ E_{20}^{-1}$ , but the actual value depends on the arrival direction of a CR particle. Cen A is only  $\sim 50^\circ$  away in longitude from the Galactic Center, and only  $\sim 20^\circ$  from the Galactic plane, while Cen B is very close  $\sim 1^\circ$  to the Galactic equator. Cosmic rays coming from either of these objects could be influenced by the stronger magnetic field near the Galactic plane (a few  $\mu\text{G}$  vs.  $\sim 1 \mu\text{G}$  in the Galactic halo) over tens of kpcs of their trajectory. This would provide a greater deflection than the relatively longer path length through the weak extragalactic magnetic field. Therefore, an association of Cen A and Cen B with more events in this region is plausible.

The UHECR source distribution is usually assumed homogeneous or to follow the baryon density distribution. The former case is relevant for energies below the photopion production threshold for proton injection where the energy losses are small and particles may come from cosmological distances. Since only a small fraction of the sky is covered with an extragalactic magnetic field capable of deflecting UHECR particles by a significant angle (Dolag et al. 2005), the resulting distri-

bution of arrival directions is close to isotropic (Takami et al. 2006). If the observed energy of CRs is near the GZK cut-off, the sources are likely local. In this case the distribution of sources traces the baryon density distribution in the local Universe and the effective field acting on UHECRs should be considerably stronger, leading to larger deflection angles. The distribution of the deflection angles depends on the details of the simulations, e.g., Sigl et al. (2004) predicts large deflection angles,  $\sim 20^\circ$  at  $10^{20}$  eV, while Dolag et al. (2005) gives much smaller angles, but allows for angles  $> 3^\circ$  in a small fraction of the sky  $< 0.01$ . Therefore, the arrival directions of UHECRs (Abraham et al. 2007b) should correlate with the distribution of large deflections on a deflection map; such a correlation can be seen even from a by-eye comparison with the deflection map given by Takami et al. (2006, their Figure 5). The sources of UHECRs should also be capable of producing lower energy CRs and  $\gamma$ -rays (and neutrinos) and, therefore, may be observed with the next generation  $\gamma$ -ray telescopes.

Most of our discussion has described the situation if the UHECRs particles are protons. This is complicated further if the injected particles are CR nuclei since the deflection angles can be larger for a given magnetic field and the nuclei undergo photodisintegration processes on the CMB and extragalactic infrared background fragmenting into lighter nuclei (e.g., Stecker & Salamon 1999). The UHECR chemical composition is unknown and subject to considerable debate. Results from the surface arrays AGASA (Shinozaki 2006) and Yakutsk (Knurenko et al. 2008) and fluorescence detectors (e.g., Sokolsky & Thomson 2007, and references therein) indicate a trend toward proton dominated composition at the highest energies. However, the Auger Collaboration has presented a fit to the elongation rate<sup>14</sup> (Unger et al. 2007) showing a heavier or mixed composition at the highest energies. These interpretations are complicated by the necessary reliance on hadronic interaction models which have to extrapolate cross section information beyond current accelerator energies, and indeed even details of the UHECR sources themselves can introduce degeneracy in the interpretation of the data with different chemical compositions (e.g., Arisaka et al. 2007). It has been argued recently (e.g., Dermer 2008; Fargion 2008; Hooper et al. 2008) that the current anisotropy results can be explained if the composition has a significant component of light nuclei,  $4 \leq A \leq 14$ , but this remains to be tested by further data.

## 5. CONCLUSION

A transition from an isotropic distribution of arrival directions of CRs above  $\sim 1$  EeV (Watson 2008) to an anisotropic distribution of the highest-energy CRs above 57 EeV (Abraham et al. 2007b) observed by Auger implies a change in the propagation mode of UHECRs in intergalactic and/or Galactic space. The association of the observed events with the supergalactic plane (Abraham et al. 2007b; Stanev 2008) points to the sources tracing the supergalactic plane and matter distribution which correlates with AGN. However, as we have shown, almost all nearby ( $d_L \leq 150$  Mpc) active galaxies found within the search radii of  $3.2^\circ$  around the UHECR events detected by Auger are typical for the local low-luminosity AGN of the Seyfert/LINER type. They are characterized by low-power and short jet activity, which is

substantially different from that observed in radio galaxies and quasars (as typically considered in the scenarios for acceleration of UHECRs). Moreover, such selected low-luminosity AGN are expected to be quite common in the local Universe, with the estimated surface density  $1.4 \times 10^3$  per steradian, when limited to a redshift  $z \leq 0.037$ . If the acceleration of UHECRs is indeed associated with jet activity, which is most likely, we conclude that the correlation with particular AGN is a coincidence. To distinguish between the persistent and episodic (e.g., Farrar & Gruzinov 2008) models of UHECR sources, future, more extensive analyzes have to take into account details of the AGN radio morphology and spectral properties, and may yield a correlation with a larger deflection angle and/or more distant sources.

We emphasize that there is no complete all-sky catalog of nearby AGN. In addition, many “regular” galaxies when studied at sufficient spatial resolution at different wavelengths show some (typically weak) level of the AGN-like activity. Hence, the confusion in classification of such sources in the literature, different databases, and catalogs. Thus, investigating the correlation of UHECRs with AGN based on some given particular AGN catalog may be tricky and even meaningless. In particular, using catalogs of X-ray selected local active galaxies (as in, e.g., George et al. 2008) may give misleading results since the X-ray emission of Seyferts and LINERs is produced by the accretion disks and the disk coroneae, and therefore represents the accretion power of the active nucleus rather than the power of its jet. Although the most recent studies have found a correlation between the disk luminosity and the radio power of the unresolved nucleus (Ho 2002; Ho & Peng 2001; Panessa et al. 2006, 2007), the former has no direct relation with the large-scale radio structures which are supposed to be capable of accelerating CRs up to the highest energies. Besides, the *present time* X-ray luminosity of the disks may have nothing to do with the *observed* UHECR events because of the considerable time delay between the arrivals of particles and photons (see §4); on the other hand, *past* UHECR acceleration activity that produced the observed UHECR events, if not episodic, has to manifest itself by extended jets that we should be able to see *now*. As argued in this paper, the spectral and morphological properties of the *jetted* AGN which are selected as likely counterparts of the detected UHECR events should be considered in detail and compared with the properties of the parent population.

Other possibilities include a few close sources with extended jet/lobe structures, such as Cen A and Cen B, and relatively large deflections due to either stronger magnetic fields or due to the presence of heavy nuclei in the flux, or more distant sources.

Observations with  $\gamma$ -ray telescopes, such as *Fermi*/LAT, HESS, MAGIC, and VERITAS may point to the *class of sources* able to accelerate particles to TeV energies, and are therefore potentially capable of accelerating particles up to EeV energies. Such sources could also produce TeV and UHE neutrinos. Taking into account the delay between the arrival times of  $\gamma$ -rays (neutrinos) and UHECRs, such observations have to be interpreted with care: UHECRs may come from sources which are not generating TeV  $\gamma$ -rays anymore, or UHECRs that are accelerated in present day  $\gamma$ -ray emitters have not had time to propagate to us, yet. Meanwhile, Cen A and Cen B are two powerful nearby radio galaxies and, if they are indeed UHECR sources,  $\gamma$ -ray observations can provide a “current” picture at the time when the CRs were emitted since the overall time delay from propagation is very short. More-

<sup>14</sup> The elongation rate is the slope  $dX_{\max}/d \log E$ , where  $X_{\max}$  is the depth of shower maximum.

over, Cen A is large enough to be resolved by  $\gamma$ -ray instruments (e.g., *Fermi*/LAT, Atwood et al. 2008; McEnery et al. 2004). Therefore, observations with  $\gamma$ -ray telescopes may provide additional clues to the origin of UHECRs.

I. V. M. acknowledges support from NASA Astronomy and Physics Research and Analysis Program (APRA) grant. Ł. S. acknowledge support by the MEiN grant 1-P03D-003-29.

T. A. P. acknowledges partial support from the US Department of Energy. C.C.C. was supported by an appointment to the NASA Postdoctoral Program at Goddard Space Flight Center, administered by Oak Ridge Associated Universities through a contract with NASA. This research has made use of the NASA/IPAC Extragalactic Database (NED) which is operated by the Jet Propulsion Laboratory, California Institute of Technology, under contract with NASA.

## REFERENCES

- Abbasi, R. U., et al. 2005, *ApJ*, 622, 910  
 Abraham, J., et al. 2007a, *Aph*, 27, 155  
 Abraham, J., et al. 2007b, *Science*, 318, 938  
 Abraham, J., et al. 2008a, *Aph*, 28, 188  
 Abraham, J., et al. 2008b, *Aph*, 29, 243  
 Alcock, C., & Hatchett, S. 1978, *ApJ*, 222, 456  
 Alvarez-Muñiz, J., Engel, R., & Stanev, T. 2002, *ApJ*, 572, 185  
 Antonucci, R. 1993, *ARA&A*, 31, 473  
 Arisaka, K., et al. 2007, *JCAP*, 12, 2  
 Atwood, W. B., et al. 2008, *ApJ*, submitted  
 Augusto, P., Wilkinson, P. N., & Browne, I. W. A. 1998, *MNRAS*, 299, 1159  
 Bahcall, J. N., Kirhakos, S., Saxe, D. H., & Schneider, D. P. 1997, *ApJ*, 479, 642  
 Baum, S. A., et al. 1993, *ApJ*, 419, 553  
 Beck, R. 2001, *Space Sci. Rev.*, 99, 243  
 Becker, R. H., White, R. L., & Helfand, D. J. 1995, *ApJ*, 450, 559  
 Beckmann, V., Gehrels, N., Shrader, C. R., & Soldi, S. 2006, *ApJ*, 638, 642  
 Begelman, M. C., Blandford, R. D., & Rees, M. J. 1984, *Rev. Mod. Phys.*, 56, 255  
 Berezhinsky, V., Gazizov, A., & Grigorjeva, S. 2006, *Phys. Rev. D*, 74, 043005  
 Biermann, P. L., & Strittmatter, P. A. 1987, *ApJ*, 322, 643  
 Bird, A. J., et al. 2007, *ApJS*, 170, 175  
 Blandford, R. D., 1990, in *Active Galactic Nuclei*, ed. T. J. L. Courvoisier & M. Mayor (Saas-Fee Advanced Course 20, Berlin:Springer), 161  
 Blasi, P., & De Marco, D. 2004, *Aph*, 20, 559  
 Bock, D. C.-J., Large, M. I., & Sadler, E. M. 1999, *AJ*, 117, 1578  
 Brinkmann, W., Siebert, J., & Bolter, Th. 1994, *A&A*, 281, 355  
 Brown, J. C., et al. 2007, *ApJ*, 663, 258  
 Burgess, A. M., & Hunstead, R. W. 2006, *AJ*, 131, 114  
 Capetti, A., et al. 1999, *ApJ*, 516, 187  
 Carilli, C. L., & Taylor, G. B. 2002, *ARA&A*, 40, 319  
 Celotti, A., & Ghisellini, G. 2008, *MNRAS*, 385, 283  
 Colbert, E. J. M., et al. 1996, *ApJ*, 467, 551  
 Condon, J. J., Helou, G., Sanders, D. B., & Soifer, B. T. 1990, *ApJS*, 73, 359  
 Condon, J. J., et al. 1998, *AJ*, 115, 1693  
 Condon, J. J., Cotton, W. D., & Broderick, J. J. 2002, *AJ*, 124, 675  
 Cordes, J. M., & Lazio, T. J. W. 2003a, preprint (arXiv:astro-ph/0207156)  
 Cordes, J. M., & Lazio, T. J. W. 2003b, preprint (arXiv:astro-ph/0301598)  
 Cronin, J. W. 2005, *Nucl. Phys. B Suppl.*, 138, 465  
 Dermer, C. D. 2007, *Proc. 30th Int. Cosmic Ray Conf. (Merida)*, in press (arXiv:0711.2804)  
 Dermer, C. D. 2008, preprint (arXiv:0804.2466)  
 Dolag, K., Grasso, D., Springel, V., & Tkachev, I. 2005, *JCAP*, 01, 009  
 Dubovsky, S. L., Tinyakov, P. G., & Tkachev, I. I. 2000, *Phys. Rev. Lett.*, 85, 1154  
 Elmouttie, M., et al. 1997, *MNRAS*, 284, 830  
 Fanaroff, B. L., & Riley, J. M. 1974, *MNRAS*, 167, 31  
 Fargion, D. 2008, *Phys. Scr.*, 78, 045901  
 Farrar, G. R., & Gruzinov, A. 2008, preprint (arXiv:0802.1074)  
 Gallimore, J. F., Baum, S. A., & O'Dea, C. P. 1997, *Nature*, 388, 852  
 Gallimore, J. F., et al. 2006, *AJ*, 132, 546  
 George, M. R., et al. 2008, *MNRAS*, 388, L59  
 Ghisellini, G., et al. 2008, *MNRAS*, 390, L88  
 Gonzalez-Martin, O., et al. 2006, *A&A*, 460, 45  
 Gorbunov, D. S., Tinyakov, P. G., Tkachev, I. I., & Troitsky, S. V. 2008, preprint (arXiv:0804.1088)  
 Gregory, P. C., Vavasour, J. D., Scott, W. K., & Condon, J. J. 1994, *ApJS*, 90, 173  
 Greisen, K. 1966, *Phys. Rev. Lett.*, 16, 748  
 Guainazzi, M., Matt, G., & Perola, G. C. 2005, *A&A*, 444, 119  
 Han, J. L. 2008, *Nucl. Phys. B (Proc. Suppl.)*, 175, 62  
 Han, J. L., et al. 2006, *ApJ*, 642, 868  
 Hao, L., et al. 2005, *AJ*, 129, 1783  
 Harari, D., Mollerach, S., & Roulet, E. 2006, *JCAP*, 11, 012  
 Haslam, C. G. T., Salter, C. J., Stoffel, H., & Wilson, W. E. 1982, *A&AS*, 47, 1  
 Helfand, D. J., Becker, R. H., White, R. L., Fallon, A., & Tuttle, S. 2006, *AJ*, 131, 2525  
 Hillas, A. M. 1984, *ARA&A*, 22, 425  
 Helou, G., Soifer, B. T., & Rowan-Robinson, M. 1985, *ApJ*, 298, 7  
 Ho, L. C. 2002, *ApJ*, 564, 120  
 Ho, L. C. 2008, *ARA&A*, in press (arXiv:0803.2268)  
 Ho, L. C., & Peng, C. Y. 2001, *ApJ*, 555, 650  
 Ho, L. C., & Ulvestad, J. S. 2001, *ApJS*, 133, 77  
 Hooper, D., Sarkar, S., & Taylor, A. M. 2008, *Phys. Rev. D*, 77, 103007  
 Hopkins, P. F., & Hernquist, L. 2006, *ApJS*, 166, 1  
 Israel, F. P. 1998, *Astron. Astrophys. Rev.*, 8, 237  
 Jones, P. A., & McAdam, W. B. 1992, *ApJS*, 80, 137  
 Jones, P. A., Lloyd, B. D., & McAdam, W. B. 2001, *MNRAS*, 325, 817  
 Karachentsev, I. D., et al. 2007, *AJ*, 133, 504  
 Kharb, P., et al. 2006, *ApJ*, 652, 177  
 Kinney, A. L., et al. 2000, *ApJ*, 537, 152  
 Knurenko, S. P., et al. 2008, *Nucl. Phys. B (Proc. Suppl.)*, 175, 201  
 Kukula, M. J., Ghosh, T., Pedlar, A., & Schilizzi, R. T. 1999, *ApJ*, 518, 117  
 Lutz, D., Maiolino, R., Spoon, H. W. W., & Moorwood, A. F. M. 2004, *A&A*, 418, 465  
 Lyutikov, M., & Ouyed, R. 2007, *Aph*, 27, 473  
 Malkan, M. A., Gorjian, V., & Tam, R. 1998, *ApJS*, 117, 25  
 Marshall, H. L., et al. 2005, *ApJS*, 156, 13  
 Martel, A. R., et al. 1999, *ApJS*, 122, 81  
 Mathis, H., et al. 2002, *MNRAS*, 333, 739  
 Mauch, T., et al. 2003, *MNRAS*, 342, 1117  
 McAdam, W. B. 1991, *Proc. Astron. Soc. of Australia*, 9, 255  
 McEnery, J. E., Moskalenko, I. V., & Ormes, J. F., 2004, in *Cosmic Gamma-Ray Sources*, eds. K. Cheng & G. E. Romero, (Dordrecht: Kluwer), *Astrophys. & Spa. Sci. Library*, v.304, 361 (arXiv:astro-ph/0406250)  
 Middelberg, E., et al. 2004, *A&A*, 417, 925  
 Molina, M., et al. 2007, *MNRAS*, 382, 937  
 Mollenhoff, C., Hummel, E., & Bender, R. 1992, *A&A*, 255, 35  
 Morganti, R., Tsvetanov, Z. I., Gallimore, J., & Allen, M. G. 1999, *A&AS*, 137, 457  
 Moshir, M., et al. 1990, *IRAS Faint Source Catalogue*, version 2.0  
 Mundell, C. G., Wilson, A. S., Ulvestad, J. S., & Roy, A. L. 2000, *ApJ*, 529, 816  
 Nagano, M., & Watson, A. A. 2000, *Rev. Mod. Phys.*, 72, 689  
 Nagar, N. M., & Wilson, A. S. 1999, *ApJ*, 516, 97  
 Nagar, N. M., Wilson, A. S., Mulchaey, J. S., & Gallimore, J. F. 1999, *ApJS*, 120, 209  
 Nagar, N. M., Falcke, H., & Wilson, A. S. 2005, *A&A*, 435, 521  
 Ostrowski, M. 1998, *A&A*, 335, 134  
 Ostrowski, M. 2002, *Aph*, 18, 229  
 Owen, F. N., Ledlow, M. J., & Keel, W. C. 1995, *AJ*, 109, 14  
 Panessa, F., et al. 2006, *A&A*, 455, 173  
 Panessa, F., et al. 2007, *A&A*, 467, 519  
 Phinney, E. S., 1983, in *Astrophysical Jets*, eds. A. Ferrari & A. G. Pacholczyk, (Dordrecht: Reidel), 201  
 Pringle, J. E., et al. 1999, *ApJ*, 526, 9  
 Roy, A. L., et al. 1998, *MNRAS*, 301, 1019  
 Rush, B., Malkan, M. A., & Edelson, R. A. 1996, *ApJ*, 473, 130  
 Sadler, E. M., Jenkins, C. R., & Kotanyi, C. G. 1989, *MNRAS*, 240, 591  
 Sambruna, R. M., et al. 2007, *ApJ*, 670, 74  
 Sanders, R. H. 1984, *A&A*, 140, 52  
 Schmitt, H. R., et al. 2001, *ApJ*, 555, 663  
 Schmitt, H. R., Pringle, J. E., Clarke, C. J., & Kinney, A. L. 2002, *ApJ*, 575, 150  
 Shinozaki, K., et al. 2006, *AJ*, 131, 2843  
 Shinozaki, K. [AGASA Collaboration] 2006, *Nucl. Phys. B (Proc. Suppl.)*, 151, 3  
 Sigl, G., Miniati, F., & Ensslin, T. A. 2004, *Phys. Rev. D*, 70, 043007

- Sikora, M., Stawarz, L., & Lasota, J.-P. 2007, *ApJ*, 658, 815
- Sokolosky, P., & Thomson, G. B. 2007, *J. Phys. G: Nucl. Part. Phys.*, 34, R401
- Sreekumar, P., et al. 1999, *APh*, 11, 221
- Stanev, T. 1997, *ApJ*, 479, 290
- Stanev, T. 2007, *Proc. 30th Int. Cosmic Ray Conf. (Merida)*, in press; arXiv:0711.2282
- Stanev, T. 2007, *Nucl. Phys. B (Proc. Suppl.)*, 168, 252
- Stanev, T. 2008, preprint (arXiv:0805.1746)
- Stanev, T., Seckel, D., & Engel, R. 2003, *Phys. Rev. D*, 68, 103004
- Stawarz, L., Kneiske, T. M., & Kataoka, J. 2006, *ApJ*, 637, 693
- Stecker, F. W. & Salamon, M. H. 1999, *ApJ*, 512, 521
- Steinle, H., et al. 1998, *A&A*, 330, 97
- Strauss, M. A., et al. 1992, *ApJS*, 83, 29
- Strong, A. W., Moskalenko, I. V., & Reimer, O. 2000, *ApJ*, 537, 763
- Svensson, R. 1996, *A&AS*, 120, 475
- Tajer, M. et al. 2005, *A&A*, 435, 799
- Takami, H., & Sato, K. 2008, preprint (arXiv:0807.3442)
- Takami, H., Yoshiguchi, H., & Sato, K. 2006, *ApJ*, 639, 803
- Thean, A., et al. 2001, *MNRAS*, 325, 737
- Ueda, Y., et al. 2005, *ApJS*, 161, 185
- Ulvestad, J. S., & Wilson, A. S. 1989, *ApJ*, 343, 659
- Ulvestad, J. S., & Ho, L. C. 2001, *ApJ*, 558, 561
- Ulvestad, J. S., Roy, A. L., Colbert, E. J. M., & Wilson, A. S. 1998, *ApJ*, 496, 196
- Ulvestad, J. S., Wrobel, J. M., & Carilli, C. L. 1999a, *ApJ*, 516, 127
- Ulvestad, J. S., et al. 1999b, *ApJ*, 517, L81
- Unger, M., et al. [Pierre Auger Collaboration] 2007, *Proc. 30th Int. Cosmic Ray Conf. (Merida)*, in press
- Urry, C. M. & Padovani, P. 1995, *PASP*, 107, 803
- Véron-Cetty, M.-P., & Véron, P. 2006, *A&A*, 455, 773
- Volonteri, M., Sikora, M., & Lasota, J.-P. 2007, *ApJ*, 667, 704
- Watson, A. A. 2008, *Nucl. Instr. Meth. Phys. Res. A*, 588, 221
- Waxman, E., & Miralda-Escudé, J. 1996, *ApJ*, 472, L89
- White, R. L., & Becker, R. H. 1992, *ApJS*, 79, 331
- Wielebinski, R., & Krause, F. 1993, *Astron. Astrophys. Rev.*, 4, 449
- Willott, C. J., Rawlings, S., Blundell, K. M., Lacy, M., & Eales, S. A. 2001, *MNRAS*, 322, 536
- Wright, A., & Otrupcek, R. 1990, *Parkes Catalog (PKS Catalog: Australia telescope national facility)*
- York, D. G., et al. 2000, *AJ*, 120, 1579
- Zatsepin, G. T., & Kuz'min, V. A. 1966, *JETP Lett.*, 4, 78
- Zdziarski, A. A., 1999, in *High Energy Processes in Accreting Black Holes*, ed. J. Poutanen & R. Svensson, *ASP Conference Series* 161, 16